# GLOBAL OBSERVATION OF FORMALDEHYDE IN THE TROPOSPHERE BY SATELLITES: GOME AND SCIAMACHY RESULTS.

**I. De Smedt[(1)], M. Van Roozendael[(1)], T. Stavrakou[(1)] , J.-F. Müller[(1)], R. Van der A[(2)], H. Eskes[(2)].**

*[(1)] BIRA-IASB, Avenue Circulaire 3, B-1180 Bruxelles, Belgium: isabelle.desmedt@aeronomie.be.*
*[(2)] KNMI, De Bilt, Netherlands: avander@knmi.nl*

## ABSTRACT

Since its launch in 1996, GOME on ERS-2 offers the possibility to observe formaldehyde ($CH_2O$) in the UV-visible range. Global distributions of $CH_2O$ columns have been derived from the whole dataset of GOME. The retrieval process is based on a slant column fitting using the differential optical absorption spectroscopy technique (DOAS), followed by a conversion to vertical column using appropriate air mass factors (AMFs). For this latter step, best-guess profiles of $CH_2O$, based on up-to-date emission inventories, atmospheric transport, photochemistry and wet/dry removal processes are provided by the 3D-CTM IMAGES. In operation since the end of 2002, SCIAMACHY provides nadir UV-visible radiance measurements suitable to complement GOME observations. New optimised DOAS settings are proposed in order to obtain a consistent time series combining the two instruments. We discuss the main error sources that affect the retrieval of both $CH_2O$ slant and vertical columns. Comparison with the tropospheric chemistry model IMAGES is used to investigate the consistency of the retrieved columns.
Tropospheric formaldehyde is a product of the air quality service of the PROMOTE\TEMIS project (ESA\GMES Service Element Atmosphere) and of the Dragon project "Air quality monitoring and forecasting in China".

## 1. INTRODUCTION

Formaldehyde ($CH_2O$) is a key component of tropospheric chemistry. It is a major by-product in the oxidation of methane as well as isoprene, the most largely emitted biogenic volatile organic compound (VOC). It is produced directly and as a secondary product during biomass burning events. It is also emitted in urban areas by oxidation of anthropogenic hydrocarbons (alkanes, alkenes, aromatics, etc.). Its photochemical removal generates CO and $HO_2$ and influences the production of tropospheric ozone. Despite its importance, there are large uncertainties in the levels and the budget of atmospheric $CH_2O$. Satellite observations of formaldehyde can help to better constrain the emissions of non-methane VOCs (NMVOCs) as well as the budget of CO in tropospheric chemical transport models (CTM).

## 2. GOME and SCIAMACHY $CH_2O$ Slant Columns Retrieval

### 2.1 Current $CH_2O$ retrievals

Several datasets of $CH_2O$ have been generated from GOME [1, 2, 3, 4]. All were retrieved using three absorption bands of $CH_2O$ between 337 and 359 nm [1, 2, 3, 4]. These results have shown that $CH_2O$ can be retrieved from satellite and be used to constrain biogenic emissions, biomass burning and also anthropogenic emissions. Current comparisons with models, for example above North America [5, 6, 7], with aircraft measurements [8, 9] and with ground-based measurements [10] give good results. GOME data have even been used to constrain VOCs emissions in tropospheric CTM models [11, 12, 13]. However, global formaldehyde columns from GOME suffer from several fitting artefacts like (1) a latitudinal dependency of the background values that need to be corrected with a reference sector method, (2) columns lower than the background level above desert regions, mainly Sahara and Australia and (3) features above oceans not predicted by 3D-CTM models like IMAGES or TM5.
Up to now, SCIAMACHY has not been much used for $CH_2O$ retrievals [14] despite the fact that it provides nadir UV-visible radiance measurements suitable to complement GOME observations. The reason is the existence of a strong polarisation anomaly that affects the SCIAMACHY spectra around 350 nm and prevents the straightforward application of the $CH_2O$ retrieval settings derived from GOME. One solution to overcome this problem is to fit $CH_2O$ further in the UV, avoiding the unwanted polarisation signature. Here we propose a new UV-shifted window suitable for both SCIAMACHY and GOME $CH_2O$ retrieval. The consistency between the new and old settings is verified using GOME spectra and the overall consistency between GOME and SCIAMACHY results is assessed.

### 2.2 Characterisation of a new UV-shifted window using GOME spectra

From inspection of the $CH_2O$ cross-sections, it can be seen that a maximum of 5 characteristic absorption bands are available in the spectral interval from 325 up to 360 nm. A compromise has to be found when defining DOAS settings, knowing that fitting accuracy is limited towards UV by the increase of the $O_3$ absorption and the resulting interference with the fit of formaldehyde (Fig. 1), while in the SCIAMACHY case,

*Proc. 'Envisat Symposium 2007', Montreux, Switzerland*
*23–27 April 2007 (ESA SP-636, July 2007)*

it is also limited towards longer wavelengths by the interference with polarisation features. Several UV-shifted fitting windows have been tested with respect to the consistency between the GOME and SCIAMACHY and the stability of $CH_2O$ slant columns. The best compromise for the number of $CH_2O$ absorption bands, the fitting errors and the need to remain under 350 nm has been found in the window 328.5-346 nm which has the advantage to include three $CH_2O$ absorption bands.

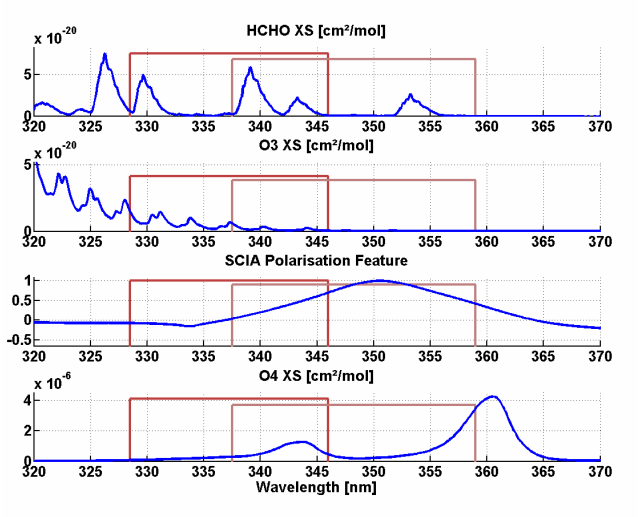


*Figure 1: $CH_2O$, Ozone, SCIAMACHY polarization signature and $O_4$ cross-sections in the near-UV.*

Despite the stronger $O_3$ absorption, the GOME slant columns appear to be improved when using this window, compared to the usual window (337.5-359 nm). Indeed, the background values above the ocean are less noisy and the values above desert regions are now at the level of the background (Fig. 2). However, the stronger $O_3$ absorption makes the reference sector method still necessary to correct the latitudinal dependency of the $CH_2O$ background level.

It is interesting to note that $CH_2O$ values retrieved using the two fitting windows are generally consistent within $2x10^{15}$ molec/cm², even above hot spots. The differences are located above desert regions and are comprised between 2 and 8 $x10^{15}$ mol/cm² (Fig. 2). Fitting residuals are lower by 15% in the tropics, but they increase more rapidly with solar zenith angle and exceed the fitting residuals of the window 337.5-359 nm poleward of 50°. Further fitting tests have shown that the artefact above desert regions disappears if the upper limit of the fitting window is kept under 350 nm and that the magnitude of the negative bias correlates with the $O_4$ absorption band peaking at 360 nm. These results suggest that the low $CH_2O$ columns above deserts are a fitting artefact, altough its exact nature could not be clearly identified here.

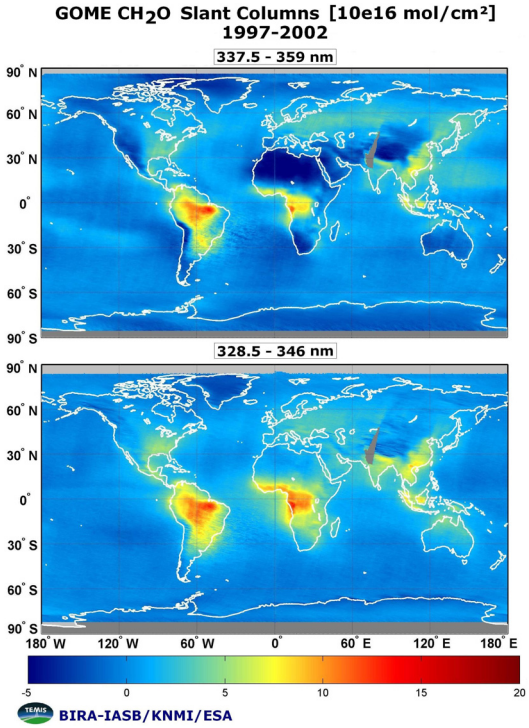


*Figure 2: GOME $CH_2O$ Slant Columns – comparison of retrievals using two fitting windows.*

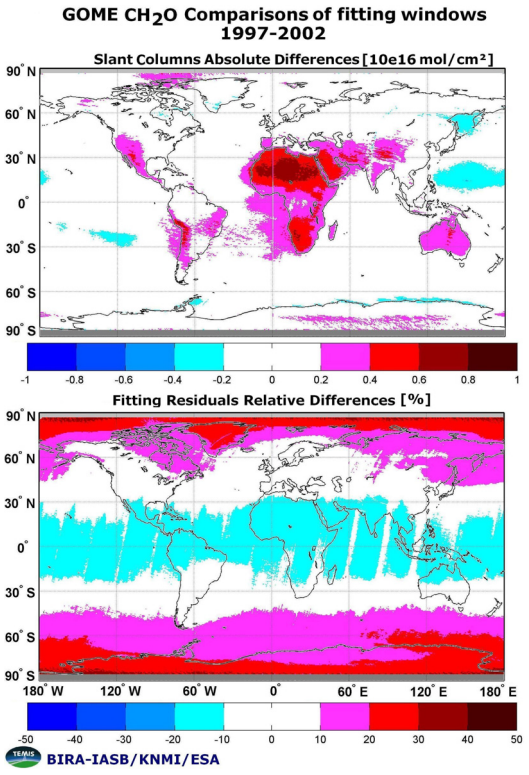


***Figure 3:*** *Differences between the two fitting windows for the GOME $CH_2O$ slant columns and the fitting residuals (6 years average).*

### 2.3 Slant Columns retrieved from SCIAMACHY

SCIAMACHY $CH_2O$ columns retrieved in the same window are found to be very consistent with the GOME columns. Among other UV-shifted fitting windows tested for SCIAMACHY, the interval 328.5-346 nm offers the lowest differences with GOME columns over the 6 first months of 2003, when the two satellite measurements overlap. Fig. 4 shows two overlapping orbits of GOME and SCIAMACHY passing over in the polluted Eastern China, on the 14 April 2003. The mean $CH_2O$ values agree very well. However, the SCIAMACHY $CH_2O$ retrieval is noisier, mainly because of its poorer signal to noise ratio. The SCIAMACHY fitting residuals are 50% higher than GOME's. With our fitting window, the dispersion of SCIAMACHY pixels is only 20% higher than GOME's, while for other tested UV-shifted windows, the dispersion is 60% higher.

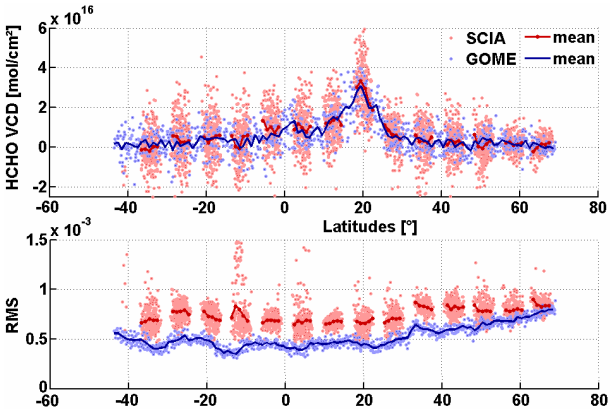


*Figure 4: GOME and SCIAMACHY orbits (14 April 2003) passing over Eastern-China.*

### 2.4 DOAS slant columns fitting parameters common for GOME and SCIAMACHY

The fitting interval and most of the settings are the same for the retrieval using GOME or SCIAMACHY spectra. The $CH_2O$ absorption cross-sections applied in the DOAS fit are those of Cantrell et al. [15] convolved to the resolution of GOME and SCIAMACHY respectively. The fitting procedure also includes reference spectra for interfering species ($O_3$, $NO_2$, BrO, and the $O_2$-$O_2$ collision). The Ring effect [16] is corrected according to Chance and Spurr [17] using a solar irradiance measured by the GOME/SCIAMACHY instrument as source spectrum. A linear intensity offset correction is further applied as well as a polynomial closure term of order 5. In order to avoid the GOME diffuser plate related artefacts [18], Fraunhofer radiance spectra are selected on a daily basis in the equatorial Pacific Ocean, in a region where the formaldehyde column is assumed to be small and stable in time. To further reduce the impact of zonal artefacts, mainly due to ozone misfits in the $CH_2O$ fitting window, an absolute normalisation is applied on a daily basis using the reference sector method [19] where the $CH_2O$ background is taken from the tropospheric 3D-CTM IMAGES [20] in the reference Pacific Ocean sector. The error on the $CH_2O$ slant columns from GOME is estimated to be 4.3 x$10^{15}$molec/cm² before 2001, while it reaches 6 x$10^{15}$molec/cm² after this date, mainly due to instrumental degradation effects affecting the signal to noise ratio of the radiance measurements. For SCIAMACHY, the noise in the measurements is higher than with GOME because of the shorter integration times used. This results in a slant column uncertainty of 6.5 x$10^{15}$molec/cm². These errors set the instrumental detection limit of formaldehyde columns.

## 3. AIR MASS FACTORS

The second step in the retrieval of tropospheric $CH_2O$ total columns is the calculation of the air mass factor that is needed to convert DOAS slant columns into corresponding vertical columns. In the troposphere, UV scattering by air molecules, clouds and aerosols makes the AMF sensitive to the vertical distribution of the absorbing molecule and to the surface albedo. Therefore air mass factors cannot be derived from straightforward geometric considerations, but instead require full multiple scattering calculations. However, if the trace gas under investigation has a small absorption optical thickness, it is possible to separate the scattering properties of the atmosphere from the vertical distribution of the absorber. The total air mass factor can then be obtained from the following expression:

$$AMF = \int_0^{TOA} w(h)S(h)dh$$

where the weighting function *w(h)* is the sensitivity of the satellite measurements to the molecule concentration at an altitude *h* and depends on the scattering properties of the observation [21]. In this work, weighting functions have been evaluated from radiative transfer calculations performed with a pseudo-spherical version of the DISORT code [22]. The scattering properties of the atmosphere have been modelled for a number of representative viewing geometries, UV-albedos and ground altitudes and stored in a look-up table. For each satellite observation, a sensitivity function is interpolated from this table. Albedos are taken from the climatology of Koelemeijer, which provides monthly Lambert-equivalent reflectivity at 335 nm [23]. The shape factor *S(h)* is the normalised profile of the absorbing molecule. Vertical shape factors are taken from the tropospheric chemistry transport model IMAGES [24] driven by analysed meteorological fields. IMAGES provides best-guess profiles of $CH_2O$ on a monthly basis, based on up-to-date emission inventories and a revised NMVOC chemistry mechanism optimized for the estimation of $CH_2O$ chemical production. The

retrieval uses the cloud top height and cloud fraction data obtained using the FRESCO cloud product [25] as delivered by KNMI on the internet web site of the TEMIS project (www.temis.nl).

Uncertainties on air mass factor calculations are dominated by uncertainties on the ground albedo, the a-priori $CH_2O$ profiles and clouds effects. For clear sky conditions and excluding the impact of aerosols not treated until now, the total error on the AMF is estimated to be around 16% while it reaches 25% for a cloud coverage of 0.5 [9]. Assuming a total vertical column of $1.5x10^{16}$mol/cm², the global error on each $CH_2O$ vertical column is estimated to be 33% (38% for cloudy pixels) for GOME and 46% (50% for cloudy pixels) for SCIAMACHY.

Fig. 5 shows the GOME $CH_2O$ vertical columns averaged over 6 years (from 1997 to 2002) and the SCIAMACHY $CH_2O$ vertical columns averaged over the next 4 years (from 2003 to 2006). The general agreement between both instruments allows the generation of a combined long-term time series of $CH_2O$ vertical columns covering a full decade from 1997 until 2006. .

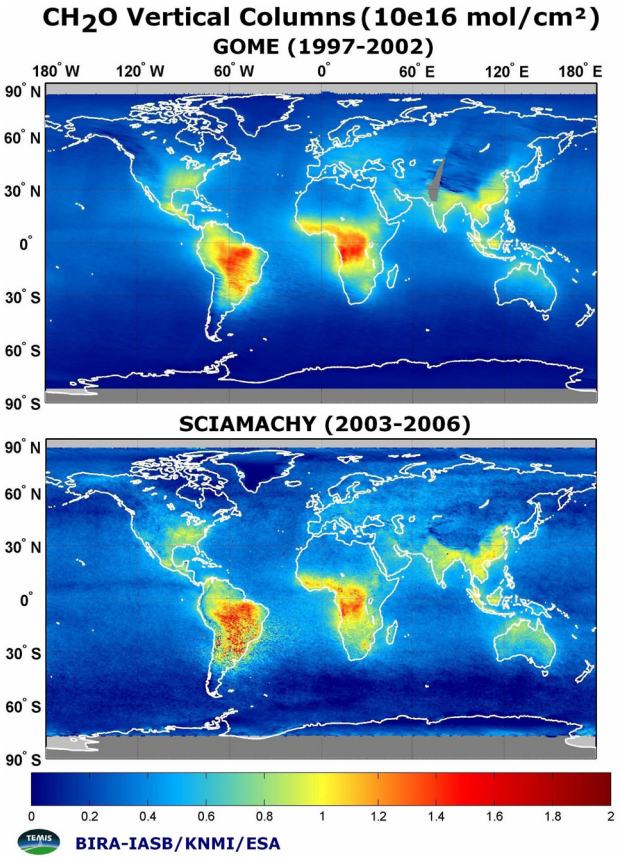


*Figure 5: $CH_2O$ vertical columns retrieved from GOME (1997-2002) and SCIAMACHY (2003-2006)*

## 4. TIME SERIES ABOVE EMISSION REGIONS AND COMPARISON WITH 3D-CTM IMAGES

Regional monthly mean $CH_2O$ values have been calculated for pixels having a cloud fraction lower than 40% and are shown in Fig. 6. The choice of other cloud fraction thresholds doesn't change significantly the monthly averages. The agreement between GOME and SCIAMACHY datasets is remarkable and shows that SCIAMACHY can be used to complete the time series of GOME despite its larger errors. Satellite data compare well with the results from the IMAGES model particularly regarding the timing of emissions. The satellite total columns are generally lower than the model over biogenic emission regions like Eastern China and in East America (North-Eastern U.S). Over biomass burning regions like Africa and Amazonia, the emission levels are very consistent. In the case of very high $CH_2O$ emissions from biomass burning like in Indonesia in 1997, satellite data do not match the high level produced by the model. Note however that the effect of aerosols has not been taken into account in the air mass factors calculation, which could have a significant impact on the retrieved total vertical columns in the case of strong fires.

*South-eastern U.S.*

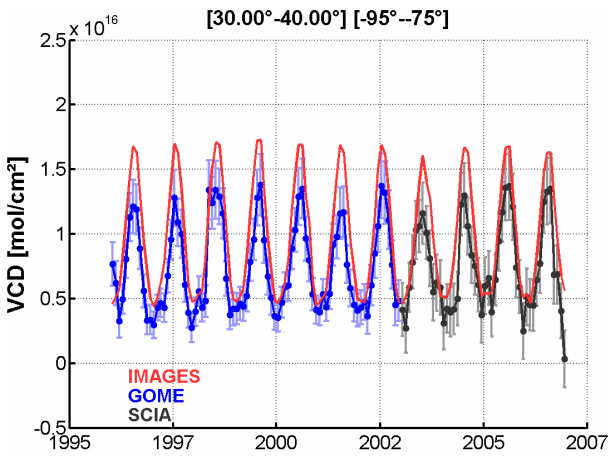


*Amazonia*

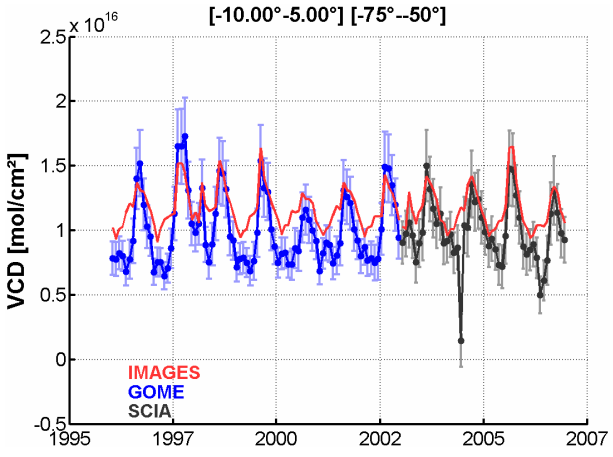

*Eastern China*

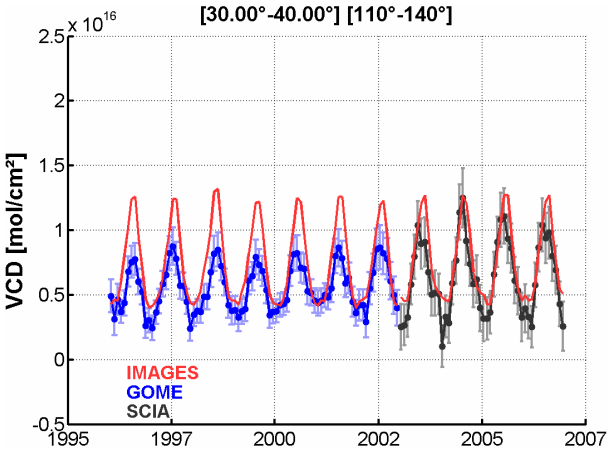


*Indonesia*

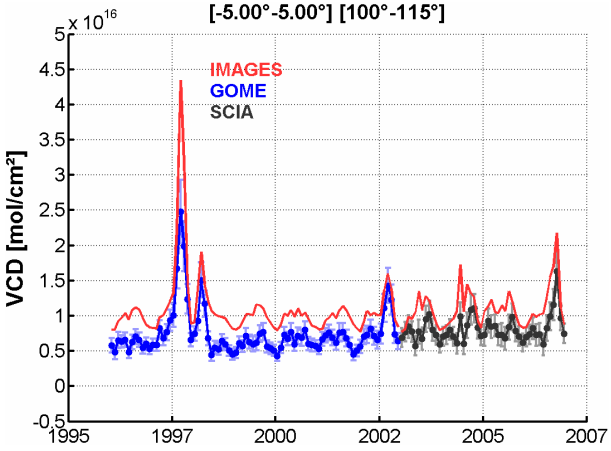


*Equatorial Africa*

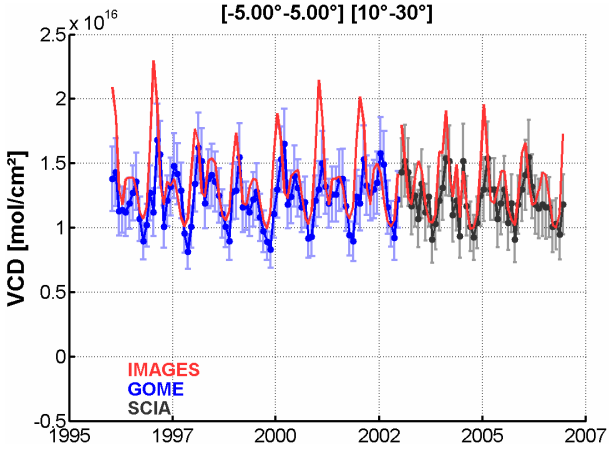


*Southern Africa*

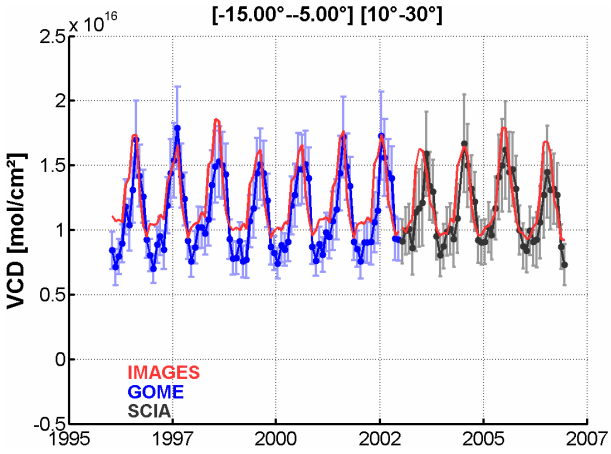


*Figure 6: Regional Monthly Mean $CH_2O$ from GOME and SCIAMACHY for cloud fraction lower than 40%. The IMAGES model is shown in red.*

## 5. CONCLUSIONS

A new fitting window has been proposed for the retrieval of $CH_2O$ from satellite measurements and has been applied to both GOME and SCIAMACHY instruments. This window allows to retrieve good quality $CH_2O$ columns from SCIAMACHY measurements despite the polarisation issue, and to overcome several fitting artefacts occurring in previous GOME retrievals. It offers the possibility to build a consistent time series of $CH_2O$ vertical columns covering the GOME and SCIAMACHY measuring periods. This dataset has been compared to simulations from the global chemistry transport model IMAGES, and may be used to provide top-down estimates for biomass burning and biogenic NMVOC emissions on the global scale.

The effect of aerosols remains to be better quantified and could have an important impact on the retrieved $CH_2O$ product in case of strong biomass burning events.

## 6. REFERENCES

1. Chance, K., P.I. Palmer, R.J.D. Spurr, R.V. Martin, T.P. Kurosu, and D.J. Jacob, Satellite observations of formaldehyde over North America from GOME, Geophys. Res. Lett., 27, 3461-3464, 2000.

2. Wittrock, F., A. Richter, A. Ladstätter-Weißenmayer, and J.P. Burrows, Global Observations of Formaldehyde, Proceedings of the ERS-ENVISAT symposium, ESA publication SP-461, 2000.

3. Marbach, T., S. Beirle, J. Hollwedel, U. Platt, T. Wagner, Identification of tropospheric emission sources from satellite observations: Synergistic use of trace gas measurements of formaldehyde (HCHO), and nitrogen dioxide ($NO_2$), Proceedings of the ENVISAT & ERS Symposium, ESA publication SP-572, 2004.

4. De Smedt, I., M. Van Roozendael, R. Van der A, H. Eskes, J.F. Müller, Retrieval of formaldehyde columns from GOME as part of the GSE PROMOTE and comparison with 3D-CTM calculations, Proceedings of the Atmospheric Science Conference, ESA, 2006.
5. Palmer, P. I., D. J. Jacob, K. Chance, R. V. Martin, R. J. D. Spurr, T. P. Kurosu, I. Bey, R. Yantosca, A. Fiore, and Q. Li, Air-mass factor formulation for spectroscopic measurements from satellites: application to formaldehyde retrievals from GOME, J. Geophys. Res., 106, 14,539-14,550, 2001.
6. Palmer, P. I., D. J. Jacob, A. M. Fiore, R. V. Martin, K. Chance, and T. P. Kurosu, "Mapping isoprene emissions over North America using formaldehyde column observations from space, " J. Geophys. Res., doi: 10.1029/2002JD002153, 2003.
7. Abbot, D. S., P. I. Palmer, R. V. Martin, K. V. Chance, D. J. Jacob, A. Guenther, "Seasonal and interannual variability of isoprene emissions as determined by formaldehyde column measurements from space," Geophys. Res. Lett., doi: 10.1029/2003GL017336, 2003.
8. Martin, R.V., D.D. Parrish, T.B. Ryerson, D.K. Nicks Jr., K. Chance, T.P. Kurosu, A. Fried, B.P. Wert, D.J. Jacob, and E. D. Sturges, "Evaluation of GOME satellite measurements of tropospheric NO2 and HCHO using regional data from aircraft campaigns in the southeastern United States," J. Geophys. Res., 109, D24307, doi: 10.1029/2004JD004869, 2004.
9. Millet, D, D.J. Jacob, S. Turquety, R.C. Hudman, S. Wu, A. Fried, J. Walega, B.G. Heikes, D.R. Blake, H.B. Singh, B.E. Anderson, and A.D. Clarke, Formaldehyde distribution over North America: Implications for satellite retrievals of formaldehyde columns and isoprene emissions, J. Geophys. Res., 2006.
10. Wittrock, F., The Retrieval of Oxygenated Volatile Organic Compounds by Remote Sensing Techniques, Thesis, Bremen University, 2006.
11. Shim, C., Y. Wang, Y. Choi, P. I. Palmer, D. S. Abbot, and K. Chance, Constraining global isoprene emissions with Global Ozone Monitoring Experiment (GOME) formaldehyde column measurements, J. Geophys. Res., 110, D24301, doi:10.1029/2004JD005629, 2005.
12. Palmer, P. I., D. S. Abbot, T-M. Fu, D. J. Jacob, K. Chance, T. Kurosu, A. Guenther, C. Wiedinmyer, J. Stanton, M. Pilling, S. Pressley, B. Lamb, and A. L. Sumner, "Quantifying the seasonal and interannual variability of North American isoprene emissions using satellite observations of formaldehyde column," J. Geophys. Res.., doi: 10.1029/2005JD006689, 2006.
13. Muller, J.F., J. Stavrakou, I. De Smedt, and M. Van Roozendael, Pyrogenic and biogenic emissions of NMVOCs inferred from GOME formaldehyde data, Proceedings of the AGU fall meeting, 2006.
14. Wittrock F., A. Richter, H. Oetjen, J. P. Burrows, M. Kanakidou, S. Myriokefalitakis, R. Volkamer, S. Beirle, U. Platt, T. Wagner, Simultaneous global observations of glyoxal and formaldehyde from space, Geophys. Res. Lett., 33, L16804, doi: 10.1029/2006GL026310, 2006.
15. Cantrell et al., Temperature-Dependent Formaldehyde Cross Sections in the Near-Ultraviolet Spectral Region, J. Phys. Chem., 94, 3902-3908, 1990.
16. Grainger, J. F. and J. Ring, Anomalous Fraunhofer line profiles, Nature, 193, 762, 1962.
17. Chance, K. and R.J.D. Spurr, Ring effect studies: Rayleigh scattering including molecular parameters for rotational Raman scattering, and the Fraunhofer spectrum, Applied Optics, 36, 5224-5230, 1997.
18. Richter and Wagner, Diffuser plate spectral structures and their influence on GOME slant columns, Tech. rep., Bremen University and Heidelberg University, 2001.
19. Khokhar, M.F., C. Frankenberg, M. Van Roozendael, S. Beirle, S. Kühl, A. Richter, U. Platt and Thomas Wagner, Satellite Observations of Atmospheric SO2 from Volcanic Eruptions during the Time Period of 1996 to 2002, Adv. Space Res., in press, 2005.
20. Müller, J.-F., and G. Brasseur, IMAGES: A three-dimensional chemical transport model of the global troposphere, J. Geophys. Res., 100, 1995.
21. Palmer, P. I., D. J. Jacob, K. Chance, R. V. Martin, R. J. D. Spurr, T. P. Kurosu, I. Bey, R. Yantosca, A. Fiore, and Q. Li, Air-mass factor formulation for spectroscopic measurements from satellites: application to formaldehyde retrievals from GOME, J. Geophys. Res., 106, 14,539-14,550, 2001.
22. Kylling, K. Stamnes and S. -C. Tsay, A reliable and efficient two-stream algorithm for spherical radiative transfer: Documentation of accuracy in realistic layered media, J. Atmos. Phys., 21, 115-150, 1995.
23. Koelemeijer, R. B. A., J. F. de Haan and P. Stammes, A database of spectral surface reflectivity in the range 335-772nm derived from 5.5 years of GOME observations, J. Geophys. Res.-Atm., 108(D2), 4070, doi: 10.1029/2002JD002429, 2003.
24. Müller, J.-F., and T. Stavrakou, Inversion of CO and NOx emissions using the adjoint of the IMAGES model, Atmos. Chem. Phys. 5, 1157-1186, 2005.
25. Koelemeijer, R. B. A., P. Stammes, J. W. Hovenier, and J. F. de Haan, Global distributions of effective cloud fraction and cloud top pressure derived from oxygen A band spectra measured by the Global Ozone Monitoring Experiment: comparison to ISCCP data, J. Geophys. Res., 107(D12), 4151, doi: 10.1029/2001JD000840, 2002.